Evaluation of meteorological observation systems on the R/V *Hi'ialakai*

2011 WHOTS-8 Field Program.

July 6 – July 13, 2011

Ludovic Bariteau[1], C. W. Fairall[2], Sergio Pezoa[2], Al Plueddemann[3], Chris Duncombe Rae[3]

1 Cooperative Institute for Research in Environmental Sciences (CIRES)

2 NOAA Earth System Research Laboratory (ESRL), Physical Sciences Division

3 Woods Hole Oceanographic Institution (WHOI)

March 19, 2012

Table of contents

1) Introduction and Goals

The R/V (Research Vessel) *Hi'ialakai* is a reconverted Tactical Auxiliary General Ocean Surveillance (T-AGOS) vessel and it is currently operated by the National Oceanic and Atmospheric Administration (NOAA) to conduct oceanographic research in the Hawaiian Islands and the Pacific Insular area. In 2011, the ship was used to support surface mooring servicing as part of the Woods Hole Oceanographic Institute (WHOI) Hawaii Ocean Time-series Station (WHOTS) project.

As part of this effort, the Earth System Research Laboratory (ESRL) Physical Science Division (PSD) Air-Sea Interaction group participated in the WHOTS-8 cruise, providing a portable flux calibration facility for calibration and intercomparison of the *Hi'ialakai*'s meteorological instruments.

In this report, we describe the meteorological sensor comparisons between the ship, the NOAA/ESRL/PSD system, and the WHOI AutoIMET system. In Section 2, the different suites of instruments used in this comparison are described. Section 3 shows the analysis procedures used for the comparison. Results and discussion are provided in Section 4. Finally, conclusions are given in Section 5.

Figure 1. Aerial view of the R/V *Hi'ialakai*.

2) Instrumentation description

a) Description of the NOAA/ESRL/PSD system

A 10-m tower was set up on the 01 deck right behind the ship's foremast (Figure 2). The fast turbulence system installed on the bow tower is composed of a Gill-Solent sonic anemometer, a Li-Cor LI-7500 fast CO_2/hygrometer, and a Systron-Donner motion-pak. A Vaisala mean temperature/humidity (T/RH) sensor in an aspirated shield and an optical rain gauge (ORG) were also mounted on the bow tower (Figure 3 left). To complete the PSD air-sea flux system, pyranometers and pyrgeometers (Eppley and Kipp&Zonen) were mounted on top of the pilot house (Figure 2). Finally, a near surface sea surface temperature (SST) sensor ('sea snake') consisting of a floating thermistor was deployed from the portside of the ship (Figure 3).

Figure 2. View of the flux tower and of the radiometers deployed on the R/V *Hi'ialakai* (red arrows).

Figure 3. Left: Close-up view of the tower and its instruments. Right: Portside view of the 'sea snake' deployment (red arrow).

The central data acquisition computer continuously logging all sources of data was located in the dry laboratory of the ship (see Figure 4). Table 1 shows sampling rates and deployment heights of the PSD sensors.

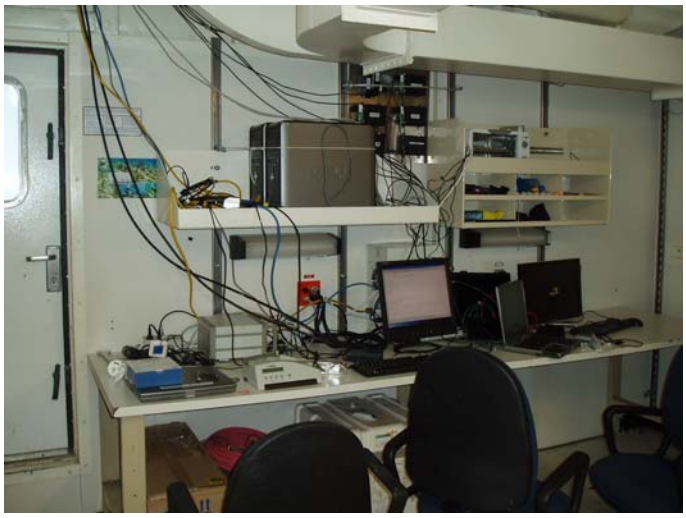

Figure 4. Location of the data acquisition system in the dry laboratory.

Table 1. PSD sensor heights and sampling rates.		
Sensor	Sampling rate	Height (m)
Sonic Anemometer	10 Hz	18
Motion Pack	10 Hz	17.8
ORG	0.1Hz, averaged to 1 sample/min	16.4
T/RH	0.1Hz, averaged to 1 sample/min	16.1
Licor (CO2&H2O)	10 Hz	16.6
Radiometers	0.1Hz, averaged to 1 sample/min	14.5
Barometer	0.1Hz, averaged to 1 sample/min	12
SST	0.1Hz, averaged to 1 sample/min	-0.05 to -0.10

b) Description of the *Hi'ialakai* system

An RM Young digital barometer and an RM Young temperature/humidity (T/RH) sensor are located on top of the pilot house (Figure 5 left). What appears to be an acoustic rain gauge mounted on top of the pressure and T/RH instruments was not reported in the SCS (Ship Computer System) data stream. The ship's RM Young anemometer used in the SCS data is mounted at the foremast (Figure 5 right). The ship's thermosalinograph (TSG) is mounted in the ship's wet laboratory and the intake is about 1.5 meters below the water line. The instrument heights and available data rate are described in Table 2. It has to be noted that the ship did not have longwave and shortwave radiometers as part of its system for WHOTS-8 cruise.

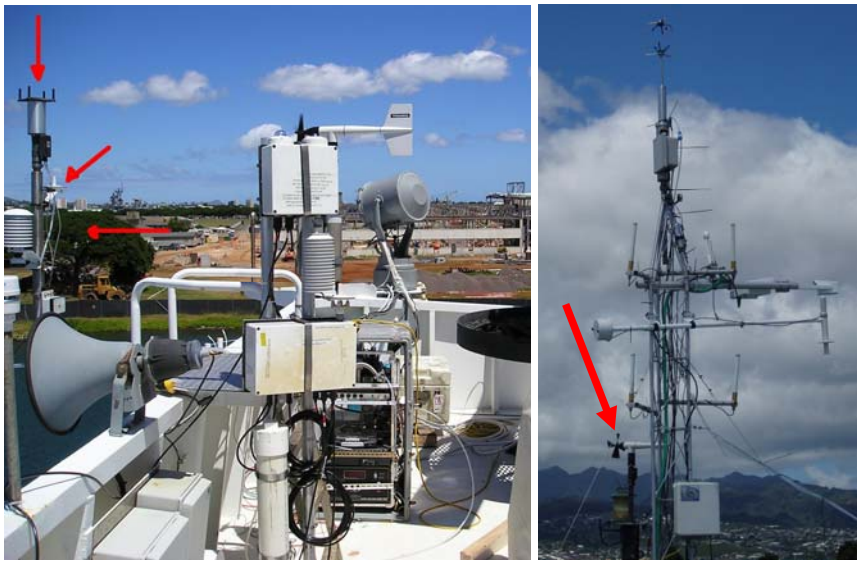

Figure 2. Left: SCS instruments on top of the wheelhouse of the *Hi'ialakai* (red arrows). Behind it is the WHOI AutoIMET system. Right: Windbird of the SCS system deployed on the foremast (indicated by red arrow).

Table 2. *Hi'ialakai* sensor heights and available data rates.		
Sensor	Available data rate	Height (m)
Anemometer	30s	15
T/RH	30s	14.5
Barometer	30s	14.5
SST (TSG)	30s	-1.5

c) Description of the AUTOimet system

An AutoIMET (AI) system from WHOI was also installed right behind the ship's instruments on top of the pilot house (Figure 6). It included a pair of radiometers (PIR/PSP), a T/RH unit (naturally ventilated shield), a barometer, a siphon raingauge and a wind sensor.

Figure 3. Back view of the AI system (red arrows) with the PSD flux mast in the background.

A description of the AI instrument heights and available data rate is given in Table 3.

Table 3. AutoIMET sensor heights and available data rates.		
Sensor	Available rate	Height (m)
Anemometer	1-minute data	14.9
Siphon rain	1-minute data	14.7
T/RH	1-minute data	14.2
PIR/PSP	1-minute data	14.8
Barometer	1-minute data	14.1

3) Method

The dual purpose of the WHOTS-8 cruise was to deploy one surface mooring (WHOTS-8) and to recover another (WHOTS-7). The R/V *Hi'ialakai* departed from Pearl Harbor, Hawaii on 6 July 2011 (Day 187) and steamed to the WHOTS site near 22º 40' N, 157º 56.8' W to first deploy the WHOTS-8 mooring (Figure 7). Afterward the ship maintained position downwind of this mooring for an intercomparison period beginning on 7-July (Day 188). Then the *Hi'ialakai* moved downwind of the WHOTS-7 mooring for another intercomparison before its recovery on 12-July (Day 192). After that, the *Hi'ialakai* returned to Pearl Harbor on July 13, 2011.

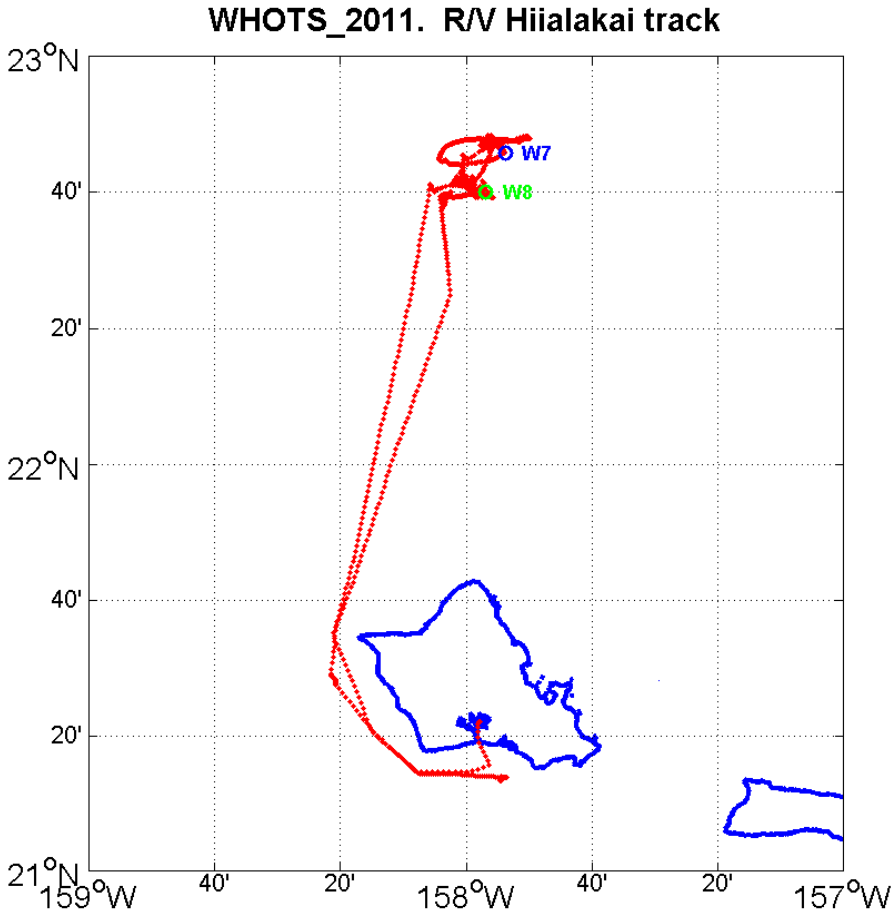

Figure 7. Cruise track of the R/V *Hi'ialakai* during WHOTS-8 cruise

The 5-min average time series of true wind speed, true wind direction (relative to North), air temperature (blue), sea surface temperature (red), incident shortwave (blue) and longwave (red), relative humidity and atmospheric pressure are shown for July 6th to July 13th (Day 187-194) in Figure 8. On this plot, we can see the sea water temperature is relatively constant around 25.1°C while the ship was stationed on the WHOTS site. The jumps in the sea temperature time series outside that time window correspond to periods when the sea snake was taken out of the water while the ship was underway or maneuvering for buoy operations. The air temperature was slightly lower than the sea temperature by 0.7°C. The winds were easterly with a speed averaging about 10 m.s^{-1}. The resulting bulk air-sea fluxes for the same dates are illustrated in Figure 9. Momentum, sensible and latent heat fluxes are computed using the COARE bulk algorithm version 3.0 (Fairall et al., 2003). The data gap around July 11th is due an acquisition issue with the radiometers and pressure datalogger.

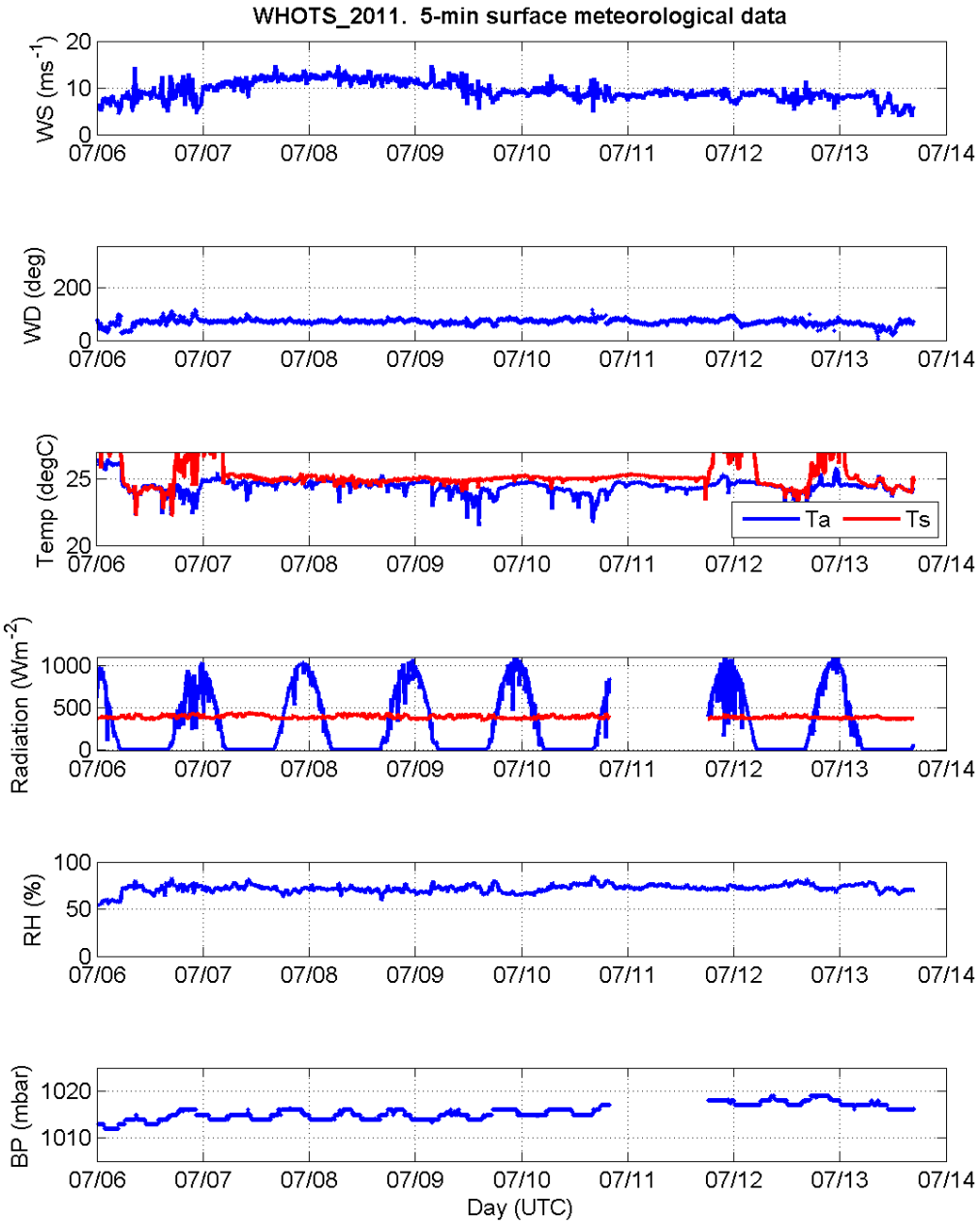

Figure 8. Meteorological conditions during WHOTS-8 from July 6th to July 13th, 2011. From the top, the panels show the wind speed ($m.s^{-1}$), the wind direction in degrees relative to North, the air temperature in blue and SST in red (°C), the incident shortwave (blue) and longwave (red) radiations ($W.m^{-2}$), the relative humidity (%) and the barometric pressure (mb).

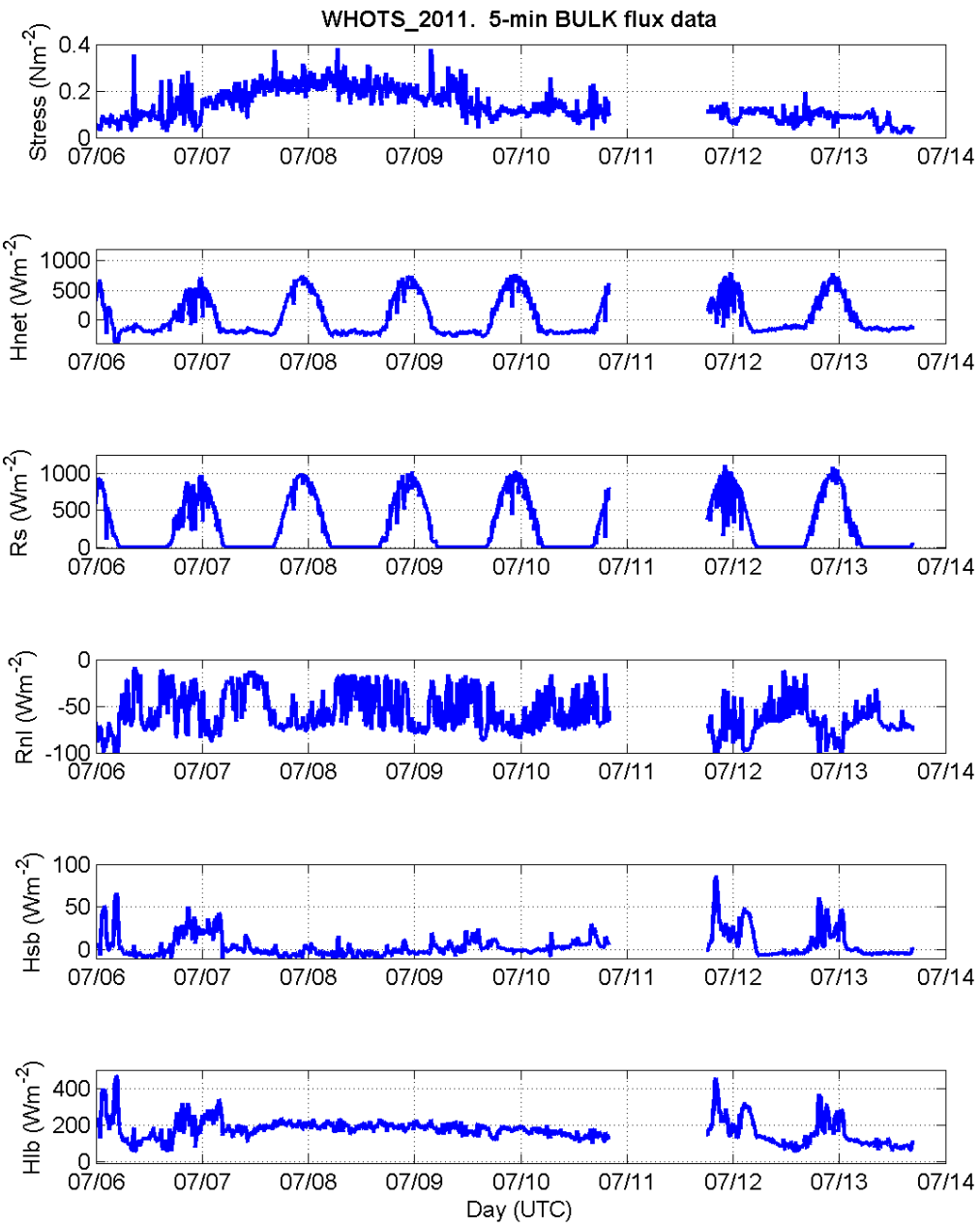

Figure 4. Bulk surface fluxes during WHOTS-8 from July 6th to July 13th, 2011. From the top, the panels show the longitudinal component of the wind stress ($N.m^{-2}$), the net heat flux ($W.m^{-2}$), the solar flux ($W.m^{-2}$), the net longwave radiation flux ($W.\ m^{-2}$), the sensible heat flux ($W.\ m^{-2}$) and the latent heat flux ($W.\ m^{-2}$).

In this report we compare the PSD, AutoIMET and ship's instruments for the intercomparison period for July 7th to July 11th (Day 188-192). Due to the difference in sensor heights and sampling strategy, the following steps were employed:

- meteorological variables were adjusted to a reference height of 10m by using the COARE3.0 bulk flux algorithm (Fairall et al., 2003). The variables adjusted at 10m are wind speed, air temperature, and relative humidity
- the PSD instruments were used as the reference for the comparisons
- standard meteorological wind direction was adopted for all of observations
- due to the disparity of sampling strategies, all the data were averaged to one-minute to match the sampling rate of the AutoIMET system.

In what follows, HA refers to *Hi'ialakai*, AI to the AutoIMET system and PSD to the NOAA/ESRL/PSD system.

4) PSD, Ship and AutoIMET comparison

In this section, we compare the various instruments installed on the *Hi'ialakai* with the PSD system used as reference. Air temperature, relative humidity and wind speed variables were all adjusted to a height of 10m.

a) Air temperature

Figure 10 shows the air temperature residual as a function of solar radiation. The residual is calculated as the difference between the instruments to evaluate minus the PSD instrument. Data were averaged into 25 W.m^{-2} bins of solar flux and the error bars are two standard deviation units in length. The Ship's T/RH sensor reads about 1.7°C too high when compared to the PSD unit, while the AI temperature sensor is in close agreement at night, but reaches about 0.5°C higher during the day. This difference is probably due to the different enclosures used (aspirated shield for PSD vs. naturally ventilated for AI) and may be exacerbated by the AI location relatively close to heated and reflective surfaces of the ship.

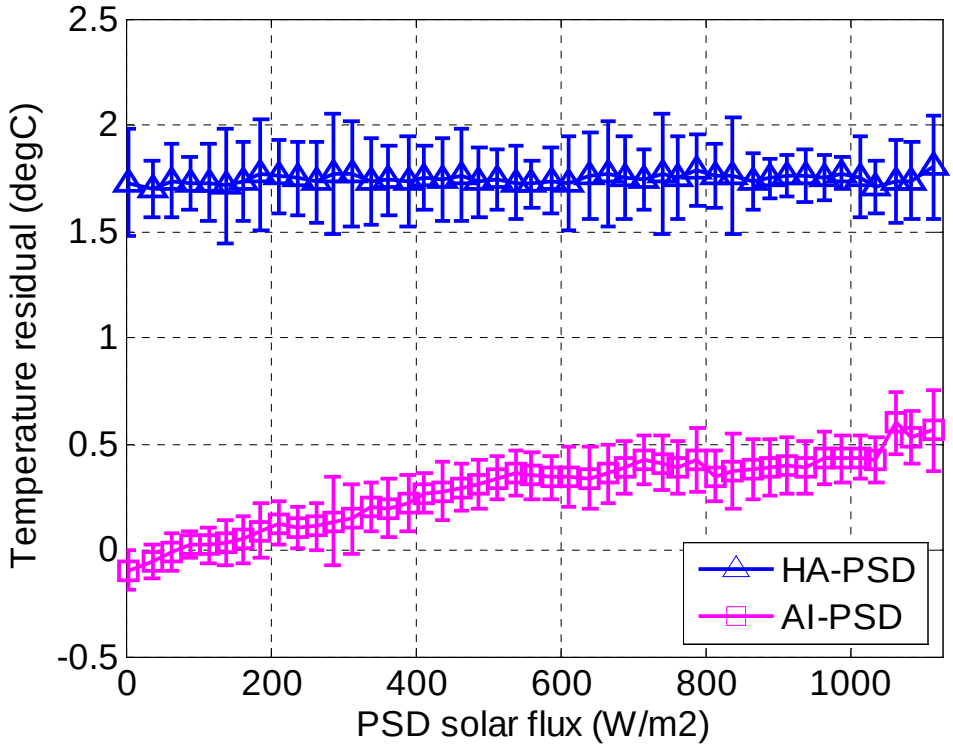

Figure 5. Dependence of air temperature residuals on solar radiation for the two ship sensors (blue and red) and the AutoIMET (magenta).

b) Relative humidity

Figure 11 shows the relative humidity residual (instrument to compare minus PSD) dependence on solar radiation for the PSD, HA and AI instruments. A correction based on post calibration was applied to the PSD humidity. As with temperature, we see that the AI is in good agreement with the PSD unit at night (~1%) but is affected by solar heating during the day and a 5% dryer air at solar peak is observed. Although the HA unit appears also to be in a naturally ventilated shield, it is a bit less sensitive to solar heating than the AI's unit and reads about 2% lower than the PSD. As with Figure 10, data were averaged into 25 $W.m^{-2}$ bins and the error bars represent two standard deviations.

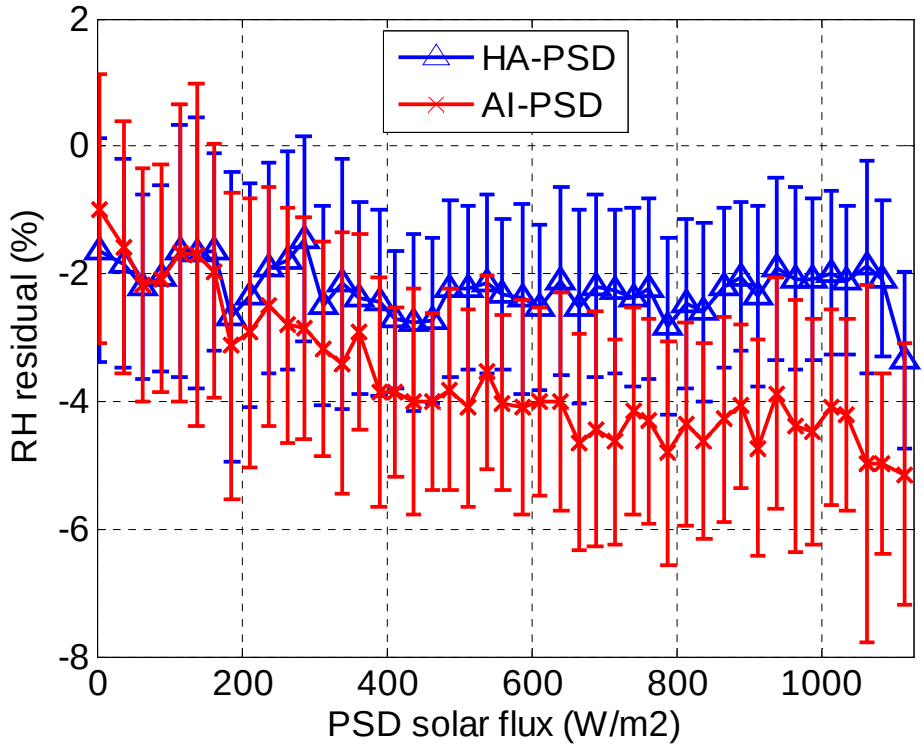

Figure 6. Relative humidity residuals as a function of solar radiation for the ship sensor (blue) and the AutoIMET (red).

c) Sea temperature

Since the AI system does not include sea surface temperature, only the ship sensor is compared to the PSD seasnake. No corrections from surface CTDs were applied to the instruments. Figure 12 shows a comparison of HA and PSD sea temperatures and shows a 0.4°C discrepancy between the two devices. To take a look closer at it, the time series of the two instruments are plotted along the measurements of WHOTS 7 and 8 buoys (Figure 13). The solar measurement is also added to it (black curve). First we note that the PSD seasnake is unusually noisy and that the small difference between the buoy readings before day 190 (July 9th) are probably due to spatial separation. Second we expect the instruments to agree relatively well at night. For visualization, we crudely added on Figure 13 an offset of 0.2°C and 0.1°C to PSD and HA respectively to make both measurements agree with the buoys at night. While this seems to reduce the discrepancy for day 191 and 192 (July 10th to July 11th), it is interesting to note that prior noon of day 190 (July 9th), PSD still appears to read lower than the buoys by about 0.1°C while the ship's thermosalinograph is slightly higher by 0.1°C.

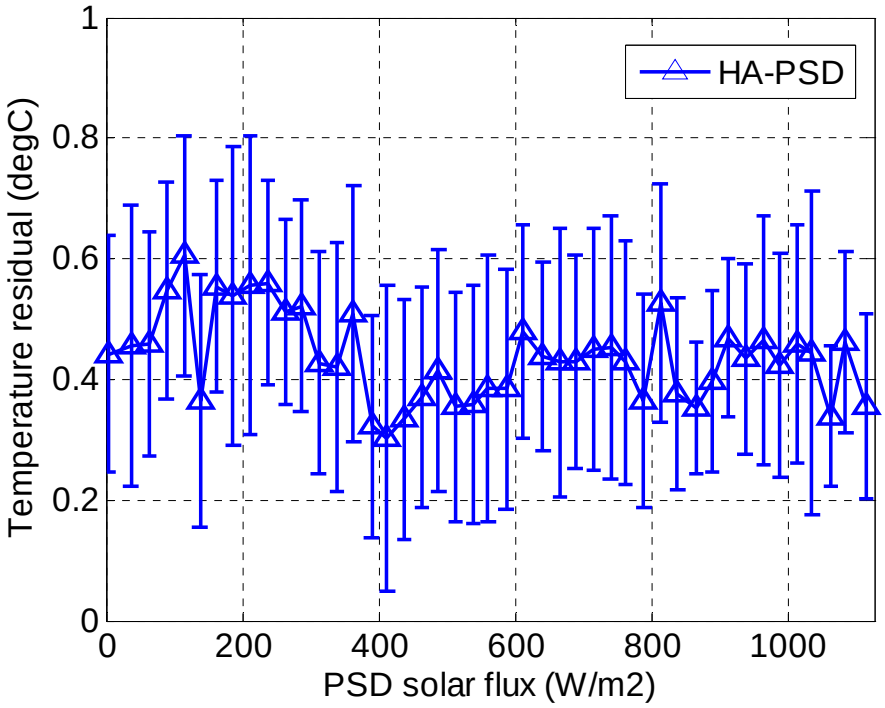

Figure 7. Dependence of sea surface temperature residual as a function of solar radiation.

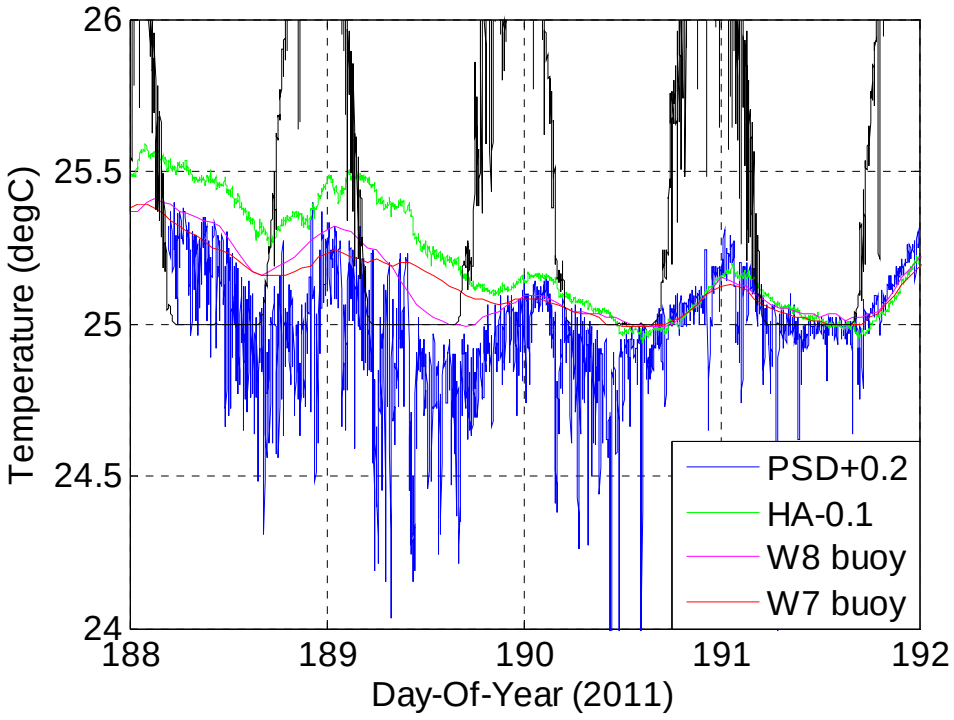

Figure 13. Sea surface temperature time series for PSD (blue), the ship sensor (green) and the two buoys (magenta and red). The back line indicates day and night periods.

d) Wind speed and direction

Wind speed residuals (instrument to compare minus PSD bow sonic) are represented as a function of relative wind direction on Figure 14. Data were averaged into one degree direction bins. Due to its location at the ship's bow, the ship propeller anemometer compares relatively well with the PSD sonic. In the (-40°, 40°) range, the ship's propeller is however affected by the flow blockage (-0. 5m.s^{-1}) resulting from the PSD tower structure behind it (see Figure 5, right picture). On top of the wheelhouse, the AI sensor is overall within 1m.s^{-1} from the PSD sonic anemometer measurement. The agreement is better when the incident wind is straight from the bow of the ship or when the flow is not too distorted by either the ship's structure or the collocated AutoIMET instruments.

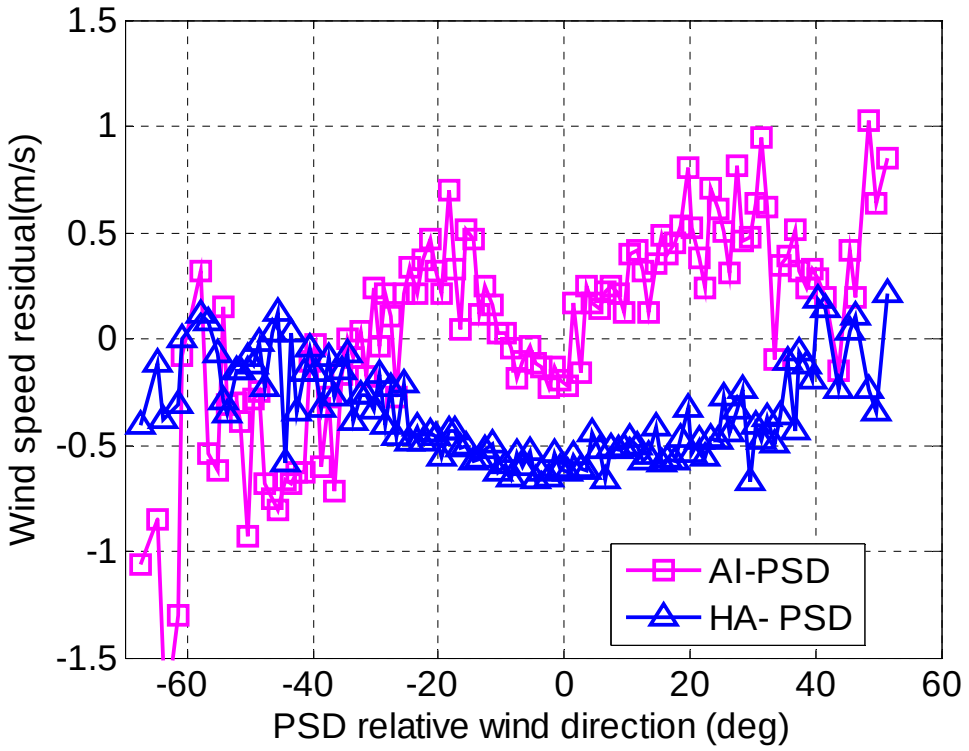

Figure 8. Wind speed residuals (instrument to compare minus PSD bow) as a function of ship relative wind direction for the ship sensor (blue) and the AutoIMET (magenta).

Figure 15 is the same as Figure 14 but for wind direction residuals (defined as instrument to compare minus PSD bow). The ship propeller anemometer agrees well with the PSD sonic in the (-70°,-5°) range but clearly deviates otherwise due to the flux tower right behind the

propeller. The AI sensor agrees well when the incident wind direction is directly over the bow of the ship but sees more dramatic direction deviations due to its deployment above the bridge roof (up to 15°).

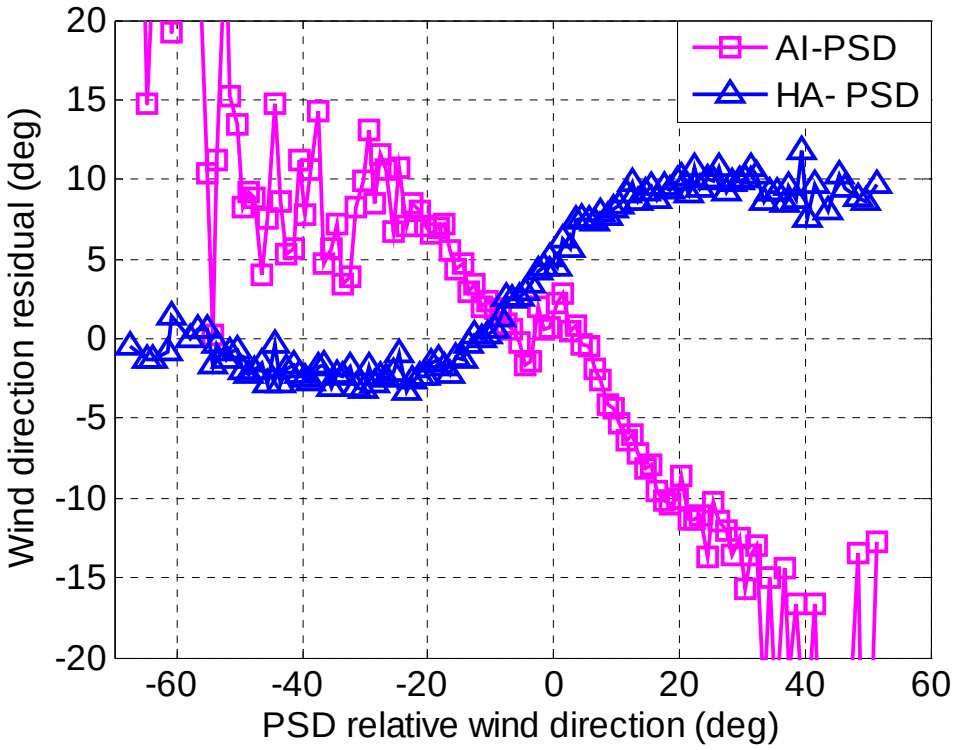

Figure 9. Wind direction residuals (instrument to compare minus PSD bow) as a function of ship relative wind direction for the ship sensor (blue) and the AutoIMET (magenta).

e) Barometric pressure

All three pressure measurements were adjusted to sea level for comparison. Because the PSD data was rounded to the nearest millibar, the residuals (instrument to compare minus PSD) are here represented as a function of pressure measured by the AI system (Figure 16 top panel). Data were averaged into one tenth of a millibar bins. The pressure difference between the PSD and AI sensors is about 0.7mb. The ship's barometer measurement has definitely a scaling issue (Figure 16 lower panel).

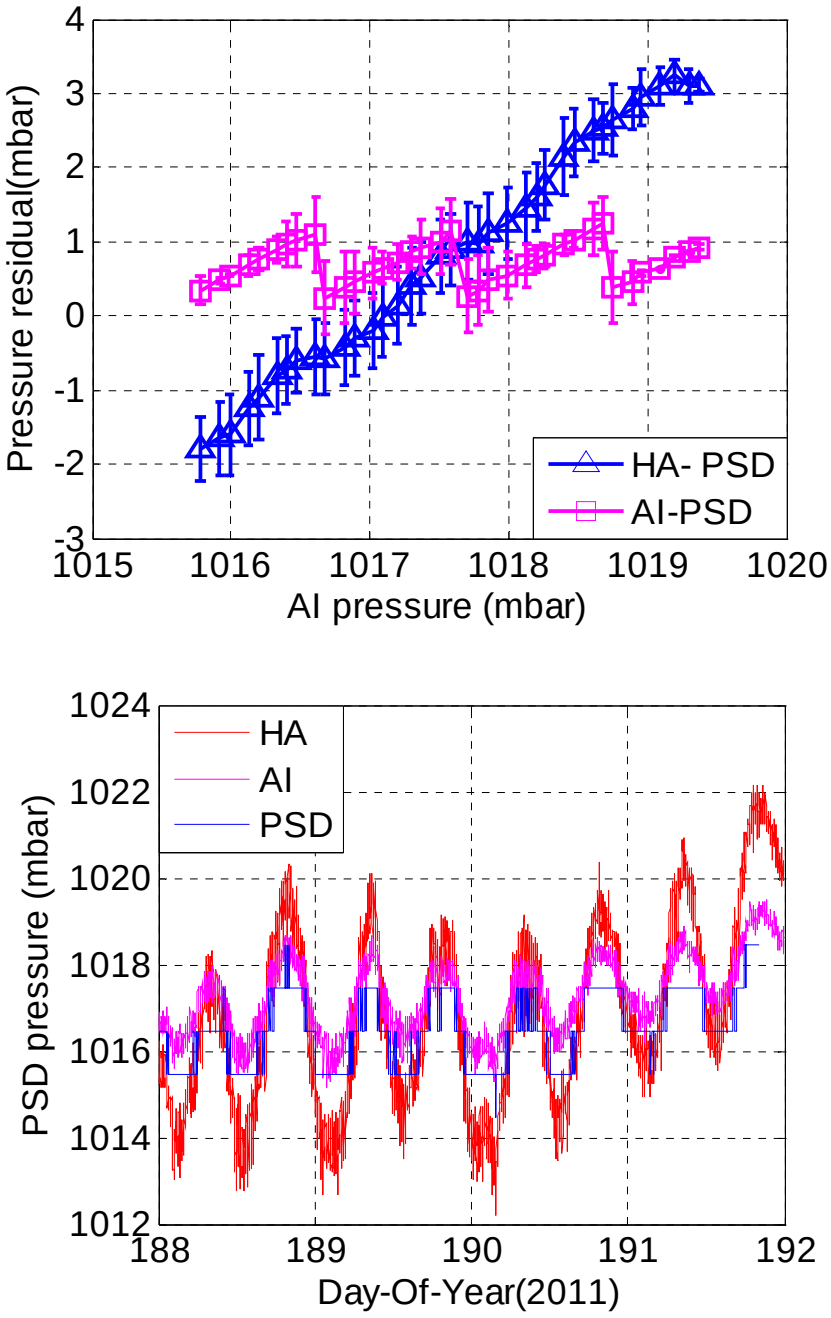

Figure 10. Upper panel: atmospheric pressure residuals (instrument to compare minus PSD bow) as a function of the AI pressure measurement for the ship sensor (blue) and the AutoIMET (magenta). Lower panel: Time series of the three measurements.

f) Longwave and shortwave radiation

Since the ship did not have longwave and shortwave radiometers as part of its system, no close-up comparison was performed in this report. We will simply show plots of the pyrgeometers and pyranometers measurements made by the PSD and AutoIMET systems (Figures 17-18). We will point out that the PSD Eppley had some anomalous dropouts that were probably associated with a bad connector but overall the agreement is good between the two PSD sensors. The AI longwave measurement had also some abnormal behavior (dropouts). A bad connector or a contamination from the ship's radar might be the cause to it. However since all three longwave sensors were deployed closely on top of the pilot house, the first reason is more likely.

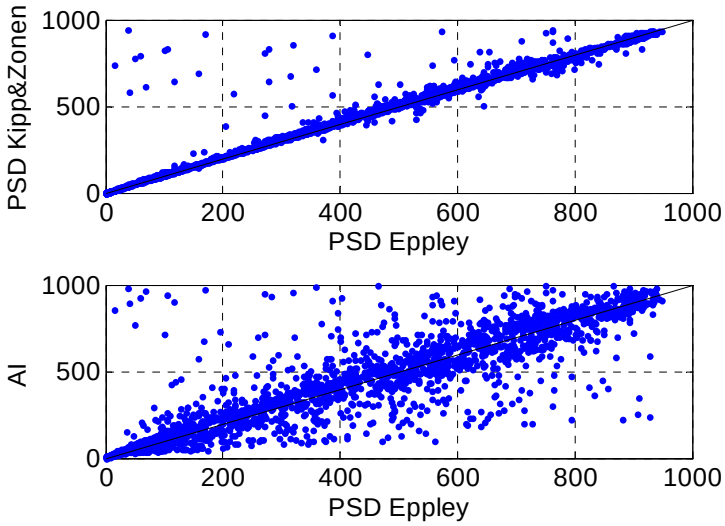

Figure 17. Comparison plots of shortwave radiation for the AutoIMET and PSD.

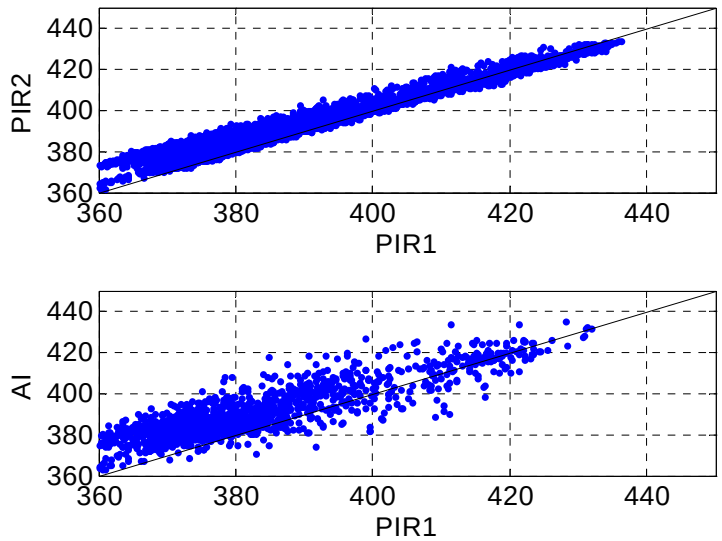

Figure 18. Comparison plots of longwave radiation for the AutoIMET and PSD.

5) Summary

An evaluation of the meteorological sensors from the *Hi'ialakai* was performed for the 2011 WHOTS-8 Field Program.

Results show that the *Hi'ialakai* air temperature unit reads about 1.7 ºC too high when compared to the PSD instrument. The AI temperature unit was found to be in very good agreement with the PSD sensor at night but reading up to 0.5 ºC higher than PSD instrument during the day. The difference is attributed to the different type of enclosure used.

Similarly the AI humidity sensor is in good agreement with the PSD unit at night but reads up to 5% higher during the day. The *Hi'ialakai* humidity sensor was a bit less sensitive to solar heating than the AI's unit and reads about 2% lower than the PSD. This difference is within accuracy limits.

The *Hi'ialakai* thermosalinograph and PSD seasnake comparison shows some inconsistency. After crude offset adjustment, both instruments have some odd behavior early in the cruise when compared to buoys.

The ship's barometer was found to have some scaling issues when compared to the AutoIMET system. The amplitude of the semi-diurnal atmospheric tide was about double the AI sensor. The pressure difference between the PSD and AI sensors was about 0.7mb.

The wind speed and direction comparisons revealed that the *Hi'ialakai* prop-vane located at the foremast is definitely setup at a good location. Distortion effects were observed but are mainly due to the PSD flux tower altering the wind flow. On the other hand, the AutoIMET unit sees more dramatic direction deviations due to its deployment above the bridge roof.

Tables 4 summarizes the comparison analyses described above, and shows the averaged differences between the different meteorological observation systems. The *Hi'ialakai* has a couple of issues to address in order to maintain the accuracy of the instruments within reasonable limits required for the SAMOS program (Fairall et al., 2007). For reference, the accuracy target estimates for this program are presented in the table 5 below, with the red values indicating improvements to be made from the 2011 WHOTS-8 Field evaluations. We recommend primarily troubleshooting the air temperature and pressure instruments and

checking calibration and flow for the TSG. Also adding shortwave and longwave measurements would be an excellent complementary to the *Hi'ialakai* meteorological system.

Table 4. Summary of differences with respect to the PSD instruments. Values left of '/' represent the average for the port side, while the right represent starboard averages.

Mean Difference with PSD	HA	AI
Air temperature (˚C)	1.7	0.28
Relative humidity (%)	-2.23	-3.62
Sea temperature (˚C)	0.4	n/a
Wind direction (deg)	-0.8 / 9	9 / -12
Wind speed (m/s)	-0.3 / -0.4	-0.2 / 0.4
Atmospheric pressure (mb)	0.8	0.7

Table 5. Accuracy targets for SAMOS

Parameter	Accuracy of Mean (bias)
Wind direction	3°
Wind speed	0.2 $m.s^{-1}$
Air Temperature	0.2 °C
Relative Humidity	2%
Atmospheric Pressure	0.1 mb
Sea Temperature	0.1 °C

References

Fairall, C. W., E. F. Bradley, J. E. Hare, A. A. Grachev, and J. B. Edson, 2003: Bulk parameterization of air-sea fluxes: Updates and verification for the COARE algorithm. J. Climate, 16, 571-591.